

Epitaxial growth of C_{60} on Ag(110) studied by scanning tunneling microscopy and tunneling spectroscopy

T. David,* J. K. Gimzewski, D. Purdie,[†] B. Reihl,[‡] and R. R. Schlittler
 IBM Research Division, Zurich Research Laboratory, CH-8803 Rüschlikon, Switzerland

(Received 3 June 1994; revised manuscript received 5 July 1994)

Using a scanning tunneling microscope, the growth of C_{60} on Ag(110) is explored. The substrate influences the natural tendency of the fullerene molecules to pack closely and an overlayer system with twofold rotational symmetry is formed: $Ag(110)c(4 \times 4)C_{60}$. This represents a distorted close-packed configuration for the C_{60} molecules, where the nearest-neighbor distance observed in bulk C_{60} is maintained. Initial island growth occurs on terrace sites away from substrate step edges, which bunch with increasing fullerene coverage. Above monolayer coverage, C_{60} grows epitaxially, maintaining twofold rotational symmetry. Tunneling spectroscopy is used to explore differences between the electronic structure in the monolayer and multilayer regimes.

Since the discovery by Krätschmer *et al.*¹ of an efficient method of preparing C_{60} molecules from graphite, extensive studies of the structural and electronic properties of this material have been carried out.² Studies have addressed both the molecular and solid states, with an increasing number concentrating on interface and adsorption phases of C_{60} . Adsorption studies on a variety of substrates have been carried out using scanning tunneling microscopy (STM). Of particular note are those that have been performed on Cu(111),^{3,4} Au(111),^{5,6} Au(110)(1×2),⁷ Au(100),⁸ and Ag(111).⁹ These, along with a number of other studies,¹⁰⁻¹² have demonstrated that there is substantial interaction between noble metal surfaces and C_{60} , probably largely driven by the propensity of C_{60} to accept electrons.

In this paper we report STM and tunneling spectroscopy (TS) results from C_{60} adsorbed on Ag(110). Specifically, we explore the role of the substrate symmetry on the initial adsorption and subsequent growth of C_{60} . Fullerene molecules normally closely pack, occupying the lattice sites of a face-centered cubic lattice and preferring the threefold (111) surface. We find that Ag(110) distorts the close packing of C_{60} molecules adsorbed on the surface. The resulting $c(4 \times 4)$ overlayer reflects the twofold symmetry of the substrate. The growth of C_{60} is in a layer-by-layer, Frank-van der Merwe,¹³ way. The shape of C_{60} islands we observe indicates that the twofold symmetry imposed by the substrate on the first layer is maintained in subsequent fullerene layers, resulting in epitaxial growth. The influence of the substrate on the crystallography of the overlayer is consistent with chemisorption of the first adsorbate layer. This involves a transfer of charge between the substrate and C_{60} , and is evidenced directly using TS.

Measurements were performed with W tips in ultrahigh vacuum using a custom-built STM operating at room temperature.¹⁴ This instrument incorporates a digital feedback loop allowing TS at fixed gap separation. The Ag(110) substrate was prepared by cycles of low energy (500 eV) Ne ion bombardment and annealing (750 K). Low energy electron diffraction and x-ray photoelectron spectroscopy were used to assess the surface order and cleanliness, respectively. Deposition of C_{60} onto Ag(110) was performed by *in vacuo*

sublimation onto a room-temperature substrate. A quartz crystal oscillator was used to control the rate of sublimation at $\sim 0.1 \text{ \AA s}^{-1}$. Deposition was followed by a short anneal (650 K, 5–10 min) before cooling the sample down to 300 K. STM topographies were acquired at a constant voltage V and tunneling current I . For the spectroscopy studies, I - V curves were recorded at various coverages to monitor the evolution of the local surface electronic structure as a function of C_{60} thickness. Each point on the I - V curves is the average value of I over multiple scans.

Figure 1(a) is an STM topograph for approximately 0.6 ML C_{60} on Ag(110). The fullerene molecules are seen to nucleate in two-dimensional (2D) islands on the terraces, with no segregation of the adsorbate towards the step edges. This is in sharp contrast to the behavior of C_{60} on Cu(111) (Ref. 3) and Ag(111),⁹ surfaces with the same symmetry as the preferred growth face of C_{60} , where nucleation is observed to occur on steps separating narrow terraces. Figure 1(b) is an STM topograph at a fullerene coverage closer to 1 ML, in which large platelettes of ordered C_{60} are observed. In the regions of bare substrate a high density of Ag steps is noted. The images in Fig. 1, and others, consistently indicate the retreat of substrate steps under the influence of the advancing edge of a growing fullerene island. These observations permit us to propose a mechanism for this substrate step bunching and provide an explanation for the observation at monolayer fullerene coverage of regular "staircases" in several regions of the surface. These staircased regions do not involve microfacetting of the surface, ruling out overannealing in the substrate preparation as their origin.

Although the structure of the fullerene monolayer, Fig. 2, resembles fcc(111), upon closer examination we observe that the distortion from this packing arrangement is significant. This is most transparent in the power spectrum representation of the STM data, shown in the inset to Fig. 2. The power spectrum is the square of the modulus of the Fourier transform of the surface, and is equivalent to the diffraction pattern of the surface. The aspect ratio of the centered rectangle in the inset to Fig. 2 corresponds to the aspect ratio of fcc(110) (to within a few percent). What we observe, therefore, is a substrate induced deformation of the lattice. In all

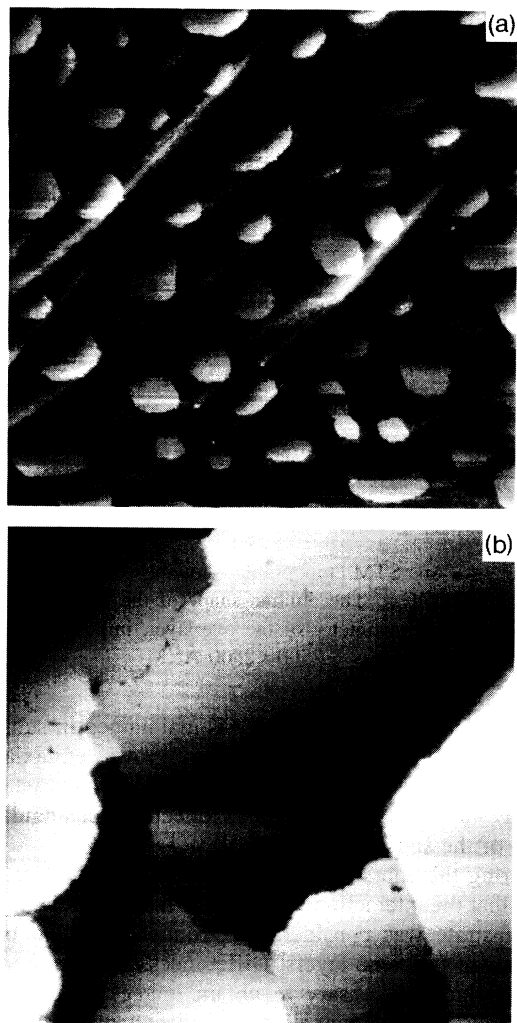


FIG. 1. (a) An STM topograph of ~ 0.6 ML C_{60} on Ag(110). Two-dimensional islands of C_{60} form on terrace sites, away from step edges of the substrate. The image size is $\sim 4000 \times 4000 \text{ \AA}^2$. (b) An STM topograph ($\sim 2000 \times 2000 \text{ \AA}^2$) showing Ag(110) with a C_{60} coverage of ~ 0.9 ML. Large, well-ordered platelettes of C_{60} are observed, with a high density of substrate steps in the interstitial regions.

our data, no suggestion of a deformation to the molecular charge density, as has been claimed occurs for the case of C_{60} adsorption on Au(100),⁸ is given.

When considering the possibilities for the growth of a material on a particular substrate there are several points of relevance. Lattice matching must be considered. It may be thought that there is a certain degree of flexibility here when considering growth of a molecular solid, but several studies have shown that C_{60} has an extremely strong tendency to maintain the intermolecular spacing and symmetry it adopts in the bulk.^{3,5-7,9,15} Ideally, lattice matching should occur over unit-cell length scales, as this minimizes the number of inequivalent adsorption sites. In addition, the reactivity of the substrate plays an important role. The preferential nucleation of C_{60} on step sites of Cu(111),³ and to a lesser extent Ag(111),⁹ substrates which provide perfect symmetry and close to ideal lattice matching over one substrate unit cell,

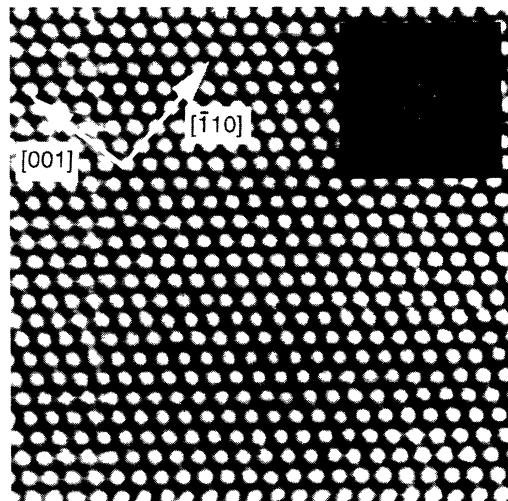


FIG. 2. An STM image ($\sim 200 \times 200 \text{ \AA}^2$) of a region at monolayer C_{60} coverage. The crystallographic directions of the substrate are marked. The inset shows the power spectrum of the main figure where the distortion of the overlayer from hexagonal symmetry is most clearly seen. The aspect ratio of the centered rectangle is equal to $\sqrt{2}$, that of fcc(110). The direction vectors refer to the substrate.

pays testimony to this. Having observed that the increased reactivity of Ag(110) over other silver surfaces acts in favor of terrace site adsorption for C_{60} , we move to consider aspects of lattice matching between Ag(110) and C_{60} . Upon comparing Ag(110) and the C_{60} lattice, we note that there is an extremely good lattice matching along $[\bar{1}10]$ of the substrate. To within $\sim 0.2\%$, three substrate unit-cell constants along $[\bar{1}10]$ span the distance between rows of lattice points along $[\bar{1}\bar{1}2]$ [which lies in the (111) plane] of the ideal C_{60} lattice. It is this lattice matching that allows C_{60} to form an ordered interface with Au(110) (Ref. 7) (gold has essentially the same lattice constant as silver). Although there are electronic differences between Au and Ag surfaces, it seems reasonable that this lattice matching should also play an important role for the adsorption of C_{60} on Ag(110). The inter- C_{60} spacing along $[\bar{1}\bar{1}2]$ (perpendicular to $[\bar{1}10]$) is 2.45 times the unit-cell constant along the $[001]$ direction of the substrate. All this suggests the formation of the overlayer shown schematically in Fig. 3(a). Here the overlayer is stretched by 2% in its $[\bar{1}10]$ direction, so that the inter- C_{60} spacing becomes 2.5 times the substrate unit-cell constant in $[001]$. Excepting the reconstruction of the substrate, this is equivalent to the (6×5) overlayer that C_{60} forms on Au(110).⁷ The C_{60} nearest-neighbor distance, marked s_{nn} in Figs. 3(a-d), is 10.07 \AA (100.3% of the bulk value), and the inter- C_{60} spacing in the $[001]$ direction of the substrate is 10.23 \AA ($\sim 102\%$ of bulk value). However, assuming no reconstruction of the substrate, this situation would necessitate three inequivalent adsorption sites, as can be seen in Fig. 3(a). Reducing this number to two, by stretching the overlayer further in its $[\bar{1}10]$ direction [Fig. 3(b)], or one, by contraction of the overlayer in $[\bar{1}10]$ [Fig. 3(c)], results in nearest-neighbor C_{60} distances of 10.6 \AA (106% of the bulk distance) and 8.2 \AA , respectively. Therefore, with this azimuthal orientation, it is clear that, in order to optimize the number of inequivalent adsorption sites, substantial demands

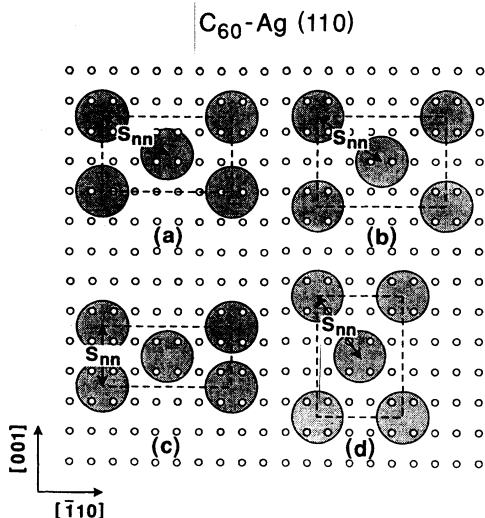


FIG. 3. Schematic diagrams showing (a–c) the three possible packing arrangements of C₆₀ on Ag(110) suggested by the extremely good lattice matching between Ag(110) and solid C₆₀ in the substrate [001] direction; and (d) the overlayer arrangement derived from our STM data, Ag(110)c(4×4)C₆₀. The small circles represent Ag atoms and the large, shaded circles fullerene molecules. The centered unit cell is marked in each case, as is the nearest-neighbor distance s_{nn} . The direction vectors refer to the substrate.

must be made on the inter-C₆₀ spacings. Experimentally, however, we find that the azimuthal orientation of the distorted hexagonal overlayer is rotated by 90° from the above models. To understand why C₆₀ adopts this unexpected azimuthal orientation, we begin by considering a 2D close-packed lattice as a centered rectangular lattice where the aspect ratio of the cell constants is $\sqrt{3}$. Changing this aspect ratio from $\sqrt{3}$ to $\sqrt{2}$, the 2D lattice becomes the (110) face of an fcc lattice (with a centered lattice point). This transformation performed on a C₆₀ close-packed monolayer, whilst maintaining the distance between the center lattice point and the corners of the lattice to be that of bulk C₆₀, changes the preferred symmetry of the adsorbate system to that of the substrate. Furthermore, the sides of the centered rectangle are (to within ~0.2%) equal to four times the Ag(110) unit cell dimensions. Therefore, by adopting the Ag(110)c(4×4)C₆₀ phase, shown schematically in Fig. 3(d), the symmetry of the substrate is entertained, the nearest-neighbor interadsorbate spacing is held essentially at the appropriate bulk value and the number of inequivalent adsorption sites is minimized.

A further strong indication of the symmetry constraints which the substrate imposes on the C₆₀ layer is shown in Fig. 4. The topograph in this figure is a large-area scan at approximately 3 ML of C₆₀ on Ag(110). If the fullerene layer was indeed growing in a close-packed formation, one would expect to observe triangular and hexagonal adsorbate islands. It is clear from the image shown in Fig. 4, however, that the island structure is oblique, and certainly not threefold symmetric. To maintain the C₆₀ coordination within the layer as high as possible, the island edges lie along the <112> directions of the substrate, explaining the observation of oblique rather than rectangular islands. Figure 4 further illustrates that the twofold rotational symmetry imposed by the sub-



FIG. 4. An STM topograph showing islands of C₆₀ on Ag(110)c(4×4)C₆₀. The oblique shape of the islands reflects the two-dimensional symmetry of the overlayer, imposed by the substrate. The scan area is ~2500×2500 Å².

strate on the first fullerene layer is maintained in subsequent layers. The fullerene crystal thus grows epitaxially on Ag(110). It is of interest to note that the islands where C₆₀ initially nucleates do not seem to reflect the rectangular symmetry of the substrate [Fig. 1(a)].

During the course of this and other¹⁶ experiments, it was noted that the interaction between the first fullerene layer and the substrate was considerably stronger than that between subsequent fullerene layers. Differences noted in the tunneling conditions necessary to obtain images of the first C₆₀ layer and those for tunneling on subsequent layers indicate that in the submonolayer coverage regime it is possible to tunnel down to tip voltages of ≤ 50 mV. We observed no evidence of contact or tip induced removal of C₆₀ in this

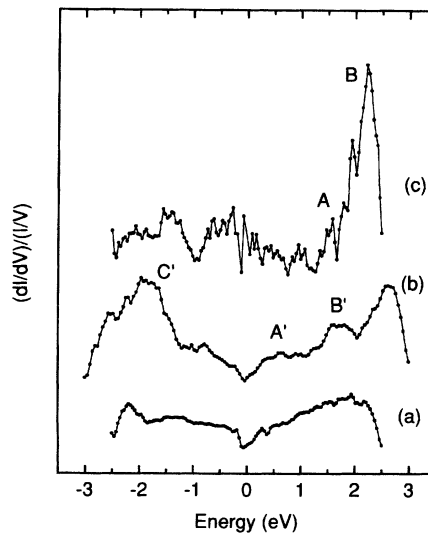


FIG. 5. Tunneling spectroscopy data from (a) Ag(110), (b) Ag(110)c(4×4)C₆₀, and (c) multilayer C₆₀ on Ag(110).

coverage regime. In contrast, when tunneling on multilayers it was found necessary to keep the tunneling voltage greater than 1 V in order to avoid contact between tip and surface. These different imaging conditions are consistent with large differences in the electronic structure between the first and subsequent layer C_{60} molecules. This is reflected in TS performed on monolayer and multilayer covered Ag(110). Figure 5 shows TS results, displayed as normalized conductance $[(dI/dV)/(I/V)]$ spectra, obtained from the clean Ag(110) substrate [Fig. 5(a)], from Ag(110)c(4×4) C_{60} (at 0.9 ML C_{60} coverage) [Fig. 5(b)], and from a multilayer coverage of C_{60} on Ag(110) [Fig. 5(c)]. Measurements for multilayer C_{60} coverage were subject to instabilities, but are nevertheless consistent with expectation. We associate the structure (A) around +1.5 eV in Fig. 5(c) with the lowest unoccupied molecular orbital of C_{60} , and the peak (B) at +2.2 eV with the second unoccupied molecular orbital.¹⁶ These features

move down towards E_F (to A' and B' , respectively) for data recorded from Ag(110)c(4×4) C_{60} [Fig. 5(b)], consistent with inverse photoemission data.¹⁶ In the occupied region, we assign the feature C' at -1.8 eV in Fig. 5(b) to the highest occupied molecular orbital of C_{60} .

In summary, we have shown that C_{60} grows in an ordered fashion on Ag(110), forming Ag(110)c(4×4) C_{60} . At the initial stages of growth, C_{60} orders on terrace sites in a distorted close packed way which accommodates the twofold rotational symmetry of the substrate. The azimuthal orientation of the overlayer is such that only a single adsorption site is required. The local environment of the C_{60} molecule is close to that adopted in the solid state. Subsequent C_{60} layers grow epitaxially, maintaining a symmetry reduced from that normally associated with bulk C_{60} . Differences in the electronic structure of the first layer of C_{60} and subsequent layers are observed with tunneling spectroscopy.

*On leave from Laboratoire d'Optique Submicronique, Université de Bourgogne, Bâtiment Mirande, BP 138, 21004 Dijon Cedex, France.

†Present address: Institut de Physique, Université de Neuchâtel, CH-2000 Neuchâtel, Switzerland.

‡Author to whom correspondence should be addressed, electronic address: brl@zurich.ibm.com

¹W. Krätschmer, L. D. Lamb, K. Fostiropoulos, and D. R. Huffman, *Nature* **347**, 354 (1990).

²G. Van Tendeloo, S. Amelinckx, M. A. Verheijen, P. H. M. van Loosdrecht, and G. Meijer, *Phys. Rev. Lett.* **69**, 1065 (1992); P. A. Heiney, J. E. Fischer, A. R. McGhie, W. J. Romanow, A. M. Denenstien, J. P. McCauley, A. B. Smith, and D. E. Cox, *ibid.* **66**, 2911 (1991); J. L. Martins, N. Troullier, and J. H. Weaver, *Chem. Phys. Lett.* **180**, 457 (1991); D. L. Lichtenberger, K. W. Nebesny, C. D. Ray, D. R. Huffman, and L. D. Lamb, *ibid.* **176**, 203 (1991).

³K. Motai, T. Hashizume, H. Shinohara, Y. Saito, H. W. Pickering, Y. Nishina, and T. Sakurai, *Jpn. J. Appl. Phys.* **32**, L450 (1993).

⁴T. Hashizume, K. Motai, X. D. Wang, H. Shinohara, Y. Saito, Y. Maruyama, K. Ohno, Y. Kawazoe, Y. Nishina, H. W. Pickering, Y. Yuk, and T. Sakurai, *Phys. Rev. Lett.* **71**, 2959 (1993).

⁵E. I. Altman and R. J. Colton, *Surf. Sci.* **279**, 49 (1992).

⁶J. K. Gimzewski, S. Modesti, Ch. Gerber, and R. R. Schlittler, *Chem. Phys. Lett.* **213**, 401 (1993).

⁷J. K. Gimzewski, S. Modesti, and R. R. Schlittler, *Phys. Rev. Lett.* **72**, 1036 (1994).

⁸Y. Kuk, D. K. Kim, Y. D. Suh, K. H. Park, H. P. Noh, S. J. Oh, and S. K. Kim, *Phys. Rev. Lett.* **70**, 1948 (1993).

⁹E. I. Altman and R. J. Colton, *Surf. Sci.* **295**, 13 (1993).

¹⁰T. R. Ohno, Y. Chen, S. E. Harvey, G. H. Kroll, J. H. Weaver, R. E. Hauffer, and R. E. Smalley, *Phys. Rev. B* **44**, 13 747 (1991).

¹¹S. J. Chase, W. S. Bacsa, M. G. Mitch, L. J. Pilione, and J. S. Lannin, *Phys. Rev. B* **46**, 7873 (1992).

¹²S. Modesti, S. Cerasari, and P. Rudolf, *Phys. Rev. Lett.* **71**, 2469 (1993).

¹³F. C. Frank and J. H. van der Merwe, *Proc. R. Soc. London Ser. A* **198**, 205 (1949).

¹⁴R. Gaisch, J. K. Gimzewski, B. Reihl, R. R. Schlittler, M. Tschudy, and W. D. Schneider, *Ultramicroscopy* **42-44**, 1621 (1992).

¹⁵G. Gensterblum, L.-M. Yu, J.-J. Pireaux, P. A. Thiry, R. Caudano, J.-M. Themlin, S. Bouzidi, F. Coletti, and J.-M. Debever, *Appl. Phys. A* **56**, 175 (1993).

¹⁶D. Purdie, H. Bernhoff, and B. Reihl (unpublished).

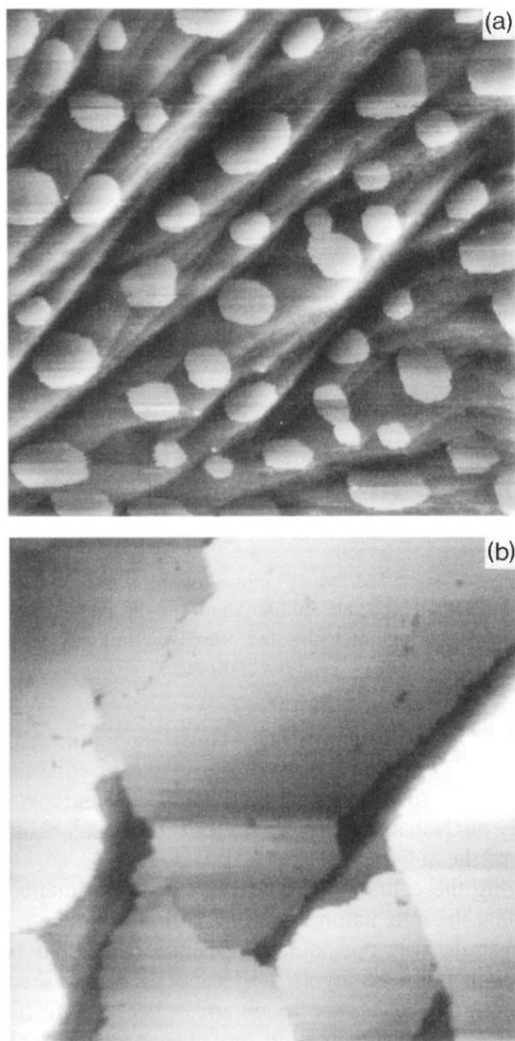


FIG. 1. (a) An STM topograph of ~ 0.6 ML C_{60} on Ag(110). Two-dimensional islands of C_{60} form on terrace sites, away from step edges of the substrate. The image size is $\sim 4000 \times 4000 \text{ \AA}^2$. (b) An STM topograph ($\sim 2000 \times 2000 \text{ \AA}^2$) showing Ag(110) with a C_{60} coverage of ~ 0.9 ML. Large, well-ordered platelets of C_{60} are observed, with a high density of substrate steps in the interstitial regions.

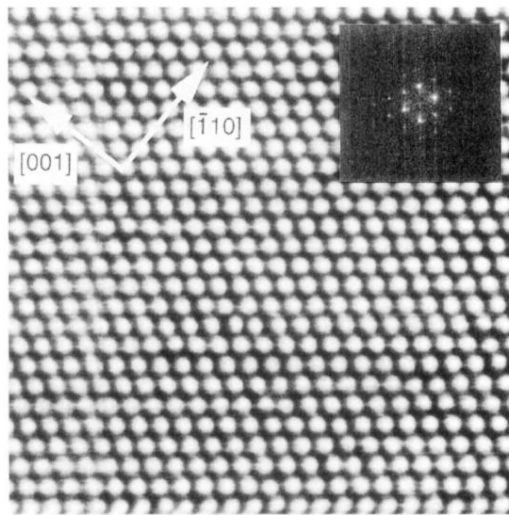


FIG. 2. An STM image ($\sim 200 \times 200 \text{ \AA}^2$) of a region at monolayer C_{60} coverage. The crystallographic directions of the substrate are marked. The inset shows the power spectrum of the main figure where the distortion of the overlayer from hexagonal symmetry is most clearly seen. The aspect ratio of the centered rectangle is equal to $\sqrt{2}$, that of fcc(110). The direction vectors refer to the substrate.

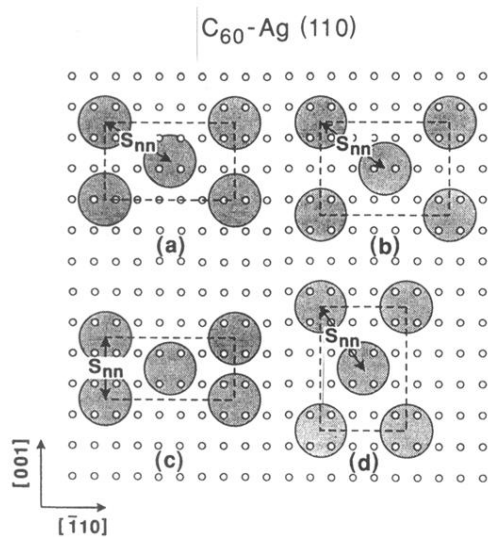


FIG. 3. Schematic diagrams showing (a–c) the three possible packing arrangements of C_{60} on Ag(110) suggested by the extremely good lattice matching between Ag(110) and solid C_{60} in the substrate $[001]$ direction; and (d) the overlayer arrangement derived from our STM data, $Ag(110)c(4 \times 4)C_{60}$. The small circles represent Ag atoms and the large, shaded circles fullerene molecules. The centered unit cell is marked in each case, as is the nearest-neighbor distance s_{nn} . The direction vectors refer to the substrate.

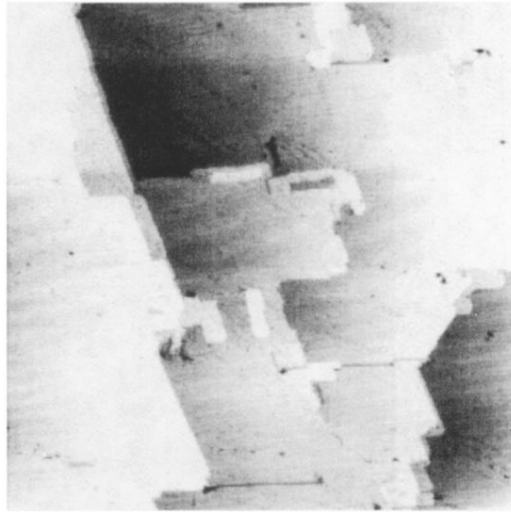


FIG. 4. An STM topograph showing islands of C_{60} on $Ag(110)c(4 \times 4)C_{60}$. The oblique shape of the islands reflects the two-dimensional symmetry of the overlayer, imposed by the substrate. The scan area is $\sim 2500 \times 2500 \text{ \AA}^2$.